RAPID COMMUNICATIONS

PHYSICAL REVIEW A VOLUME 52, NUMBER 3 SEPTEMBER 1995

Probe-transmission spectrum of a blue-detuned optical lattice

J. Guo and J. Cooper

JILA, University of Colorado and National Institute of Standards and Technology, Boulder, Colorado 80309-0440

(Received 25 April 1995)

The probe-transmission spectrum of a one-dimensional optical lattice is calculated. The optical lattice consists of atoms that are cooled by a pair of counterpropagating, linearly polarized fields, whose frequency ω is detuned to the blue side of an atomic transition. A weak probe field of frequency ω' is assumed to be propagating in the same direction as one of the cooling fields. It is shown that, owing to the existence of dark and gray states in the lattice, the probe-transmission spectrum exhibits interesting features that are qualitatively different from those of a "normal" optical lattice with red-detuned cooling fields. Examples of these features include subrecoil linewidths and reversed absorption-amplification sidebands. It is shown that by monitoring the magnitudes of resonance signals in the spectrum, one can gain information on the evolution of the dark-state population in the lattice.

PACS number(s): 32.80.Pj, 42.65.−k

In an optical lattice, an atomic vapor is cooled by a number of incident fields whose polarization vectors are orthogonal to each other. The vapor atoms can become trapped in the periodic light-shift potential wells induced by the cooling fields, and form a spatial lattice distribution. In most of the experimental realizations of optical lattices [1–5], the cooling field frequency is detuned to the red side of an atomic transition between the ground and excited states having angular momenta F and $F+1$, respectively. In such cases, the positions of the light-shift potential minima correspond to the antinodes of the field intensity, and the atoms that are trapped near these potential minima scatter photons from the cooling field at a rate determined by the optical pumping rate Γ'. Nonlinear spectroscopy has proved to be an effective way for investigating the characteristics of these red-detuned lattices; e.g., oscillation frequencies of the atoms in the potential wells, motional damping constants, paramagnetism, etc. There have been a series of probe-transmission and four-wave-mixing experiments in one-dimensional (1D) and multidimensional lattices [1–4,6,7]. Due to computational limitations, theories of nonlinear spectroscopy in optical lattices are limited to 1D [8,9] and 2D cases [10] only, and the calculated results are in qualitative agreement with some existing experiments.

If the atomic vapor density in a red-detuned lattice is sufficiently high, the photon scattering processes will result in a significant long-range dipole-dipole interaction between the atoms, which limits the effects of cooling and hinders any attempt to further increase the vapor density in the optical lattice. Recently, there has been considerable interest in the so-called blue-detuned lattices, in which the cooling fields are detuned to the blue side of an atomic $F\rightarrow F$ or $F\rightarrow F-1$ transition [11]. In this case, the minima of the light-induced potential wells correspond to the intensity nodes of the field, and the atoms that are trapped near these minima scatter photons at a rate much lower than Γ'. As a result, the mutual interaction between the atoms is expected to become weaker as compared to the case of red-detuned lattices. Furthermore, the atomic momentum distribution width can become much narrower than the photon recoil momentum $\hbar k$ (subrecoil cooling), owing to the existence of certain velocity-selective dark or gray states in the lattices, in which the atoms absorb no light or very little light from the cooling field [12].

With the ongoing experimental efforts to realize the blue-detuned lattices, it is interesting to know whether one can similarly study the properties of these lattices by nonlinear spectroscopy. In this Rapid Communication, the probe transmission spectrum of a 1D blue-detuned lattice is presented. The calculated signal exhibits novel features that are not found in the spectra of red-detuned lattices, and by studying these features, one can monitor the accumulation of the dark-state population in the lattice.

One considers the 1D model of a blue-detuned lattice first proposed by Shahriar *et al.* and Marte *et al.* [13,14]. The atomic level scheme is chosen as a $F_g=1\rightarrow F_e=1$ transition with a Bohr frequency ω_0. The cooling field having a frequency ω consists of a pair of counterpropagating, linearly polarized fields, whose polarization vectors are at an angle θ with each other. This particular configuration has the feature of combining both the polarization-gradient cooling and the velocity-selective coherent population trapping (VSCPT) mechanisms. In addition to the cooling field, a probe field of frequency ω' can be present, and is assumed to be propagating along the cooling field direction given by z. The total field in the lattice can be written as

$$\mathbf{E}=\frac{\mathscr{E}}{\sqrt{2}}e^{-i\omega t}[-\cos(kz-\theta/2)+\epsilon\eta_+e^{ikz-i\delta t}]\boldsymbol{\epsilon}_+ + \frac{\mathscr{E}}{\sqrt{2}}e^{-i\omega t}[\cos(kz+\theta/2)+\epsilon\eta_-e^{ikz-i\delta t}]\boldsymbol{\epsilon}_- + \text{c.c.}\ , \tag{1}$$

where $\delta=\omega'-\omega$ is the probe-pump detuning, $\epsilon\ll 1$, is the ratio between the strengths of the probe and cooling fields, and $\eta_\pm$ are the $\sigma^\pm$ components of the probe field polarization vector. One assumes a weak field limit defined by

$$\chi\ll\Gamma,\Delta\ , \tag{2}$$

where $\chi=d\mathscr{E}/\sqrt{2}\hbar$ is the cooling field Rabi frequency, Γ is the atomic excited-state decay rate, and $\Delta=\omega-\omega_0$ is the

cooling field detuning. In this limit, one can adiabatically eliminate the electronic excited state of the atom. The resulting master equation for the atomic ground-state density matrix ρ is given by

$$\dot{\rho}=1/i\hbar\,[H,\rho]+[\dot{\rho}]_{relax}\ , \tag{3}$$

where the Hamiltonian H can be written as

$$H=H^{(0)}+\epsilon[H^{(1)}e^{-i\delta t}+\text{H.c.}]\ . \tag{4}$$

The zeroth-order Hamiltonian, $H^{(0)}$, describes the motion of the atoms in the light-induced potential wells. It is given by [14]

$$H^{(0)}=p^2/2M+U_0[\cos^2(kz+\theta/2)|+\rangle\langle+|+\cos^2(kz-\theta/2)|-\rangle\langle-|+\cos(kz+\theta/2)\cos(kz-\theta/2)(|+\rangle\langle-|+|-\rangle\langle+|)], \tag{5}$$

where the potential depth $U_0=\Delta\chi^2/(\Gamma^2/4+\Delta^2)$, and $|\pm\rangle$ denote the magnetic sublevels $|m_g=\pm1\rangle$. The modification to the Hamiltonian due to the addition of the weak probe field, $H^{(1)}$, is given by

$$H^{(1)}=\frac{U_0}{\sqrt{2}}[\,\eta_-\cos(kz+\theta/2)|+\rangle\langle+|-\eta_+\cos(kz-\theta/2)|-\rangle\langle-|-\eta_+\cos(kz+\theta/2)|+\rangle\langle-|+\eta_-\cos(kz-\theta/2)|-\rangle\langle+|]e^{ikz-i\delta t}+\text{H.c.} \tag{6}$$

The relaxation of the density matrix ρ due to optical pumping, $[\dot{\rho}_{relax}]$, is given by

$$[\dot{\rho}]_{relax}=-\frac{\Gamma'}{2}[A\rho+\rho A]+\Gamma'\int dp'\sum_{Q=\pm}N_Q(p')\times B_Q^{\dagger}e^{-ip'z}\rho e^{ip'z}B_Q\ , \tag{7}$$

where the optical pumping rate $\Gamma'=\Gamma\chi^2/(\Gamma^2/4+\Delta^2)$. The operators A and B in Eq. (7) can be similarly expressed as

$$\begin{aligned}A&=A^{(0)}+\epsilon[A^{(1)}e^{-i\delta t}+\text{H.c.}]\ ,\\ B_Q&=B_Q^{(0)}+\epsilon[B_Q^{(1)}e^{-i\delta t}+\text{H.c.}],\end{aligned} \tag{8}$$

where $A^{(1)}$ and $B_Q^{(1)}$ represent modifications to the optical pumping rates in the presence of the probe field. The detailed expressions for A and B_Q will be presented elsewhere. The functions $N_Q(p')$ in Eq. (7) are the probability distribution functions for the emission of a spontaneous photon with a polarization component Q and a momentum $\hbar p'$ in the z direction [9].

The atomic density matrix ρ can be similarly written as

$$\rho=\rho^{(0)}+\epsilon[\rho^{(1)}e^{-i\delta t}+\text{H.c.}]\ , \tag{9}$$

and the probe transmission coefficient is given in terms of $\rho^{(1)}$ as

$$S(\delta)=\text{Im}\left\{\frac{1}{i\Gamma/2-\Delta}\text{Tr}[\rho^{(1)}(\,\eta_-^*\cos(kz+\theta/2)|+\rangle\langle+|-\eta_+^*\cos(kz-\theta/2)|-\rangle\langle-|+\eta_-^*\cos(kz-\theta/2)|+\rangle\times\langle-|-\eta_+^*\cos(kz+\theta/2)|-\rangle\langle+|)e^{-ikz}]\right\}, \tag{10}$$

where the trace is over the atomic internal and motional states. From here on, it is assumed that the angle $\theta=\pi/4$, which gives rise to optimal cooling effects.

Equation (3) can be solved in the eigenstate basis of the zeroth-order Hamiltonian $H^{(0)}$, i.e., the Bloch states $|n,q\rangle$, where n is the band index, and $q\in[-k,k)$ is the Bloch index. To zeroth order in the probe field strength, and assuming the secular limit $\Delta/\Gamma\gg1$, one can neglect the coherences between the Bloch states of different band indices n. In this case, the only nonvanishing terms of the density matrix $\rho^{(0)}$ are the populations of the Bloch states, $\pi_{n,q}=\langle n,q|\rho^{(0)}|n,q\rangle$, and Eq. (3) in the absence of the probe field reduces to a set of rate equations for $\pi_{n,q}$ [14]. It is assumed that the strength of the probe field is sufficiently weak that its effect on cooling is negligible. Starting from an arbitrary distribution of $\pi_{n,q}$ at $t=0$, one can integrate these rate equations to obtain the value of $\rho^{(0)}(t)$. As described in Ref. [14], the initial period of cooling is dominated by the more efficient polarization-gradient mechanism, and the rate for the evolution of the density matrix $\rho^{(0)}$ is on the order of a fraction of Γ'. After a cooling time of order $\Gamma' t=100$, the atomic density matrix reaches a quasistationary value with respect to polarization-gradient cooling. The population-trapping mechanism then slowly reduces the atomic momentum distribution width to below $\hbar k$. The evolution of the density matrix during this subrecoil cooling period is now characterized by a rate γ_{VSCPT}, which is three orders of magnitude smaller than Γ'. One assumes that the probing periods are sufficiently short that the changes in the zeroth-order density matrix $\rho^{(0)}$ during these periods can be neglected, but are sufficiently long for the probe-induced coherences to reach their steady-state values. This requirement can be satisfied since, as indicated below, the relaxation rates of the probe-induced coherences are on the order of a few percent of Γ'.

The equation for the first-order density matrix, $\rho^{(1)}$, can be obtained upon substitution of $\rho^{(0)}(t)$ into Eq. (3) as

$$\dot{\rho}^{(1)}=\frac{1}{i\hbar}([H^{(0)},\rho^{(1)}]+[H^{(1)},\rho^{(0)}])-\frac{\Gamma'}{2}[A^{(0)}\rho^{(1)}+\rho^{(1)}A^{(0)}+A^{(1)}\rho^{(0)}+\rho^{(0)}A^{(1)}]+\Gamma'\int dp'\sum_Q N_Q(p')\times[(B_Q^{(0)})^{\dagger}e^{-ip'z}\rho^{(1)}e^{ip'z}B_Q^{(0)}+(B_Q^{(1)})^{\dagger}e^{-ip'z}\rho^{(0)}e^{ip'z}B_Q^{(0)}]\ . \tag{11}$$

The steady-state probe-induced coherences $\rho^{(1)}(n,n',q)$

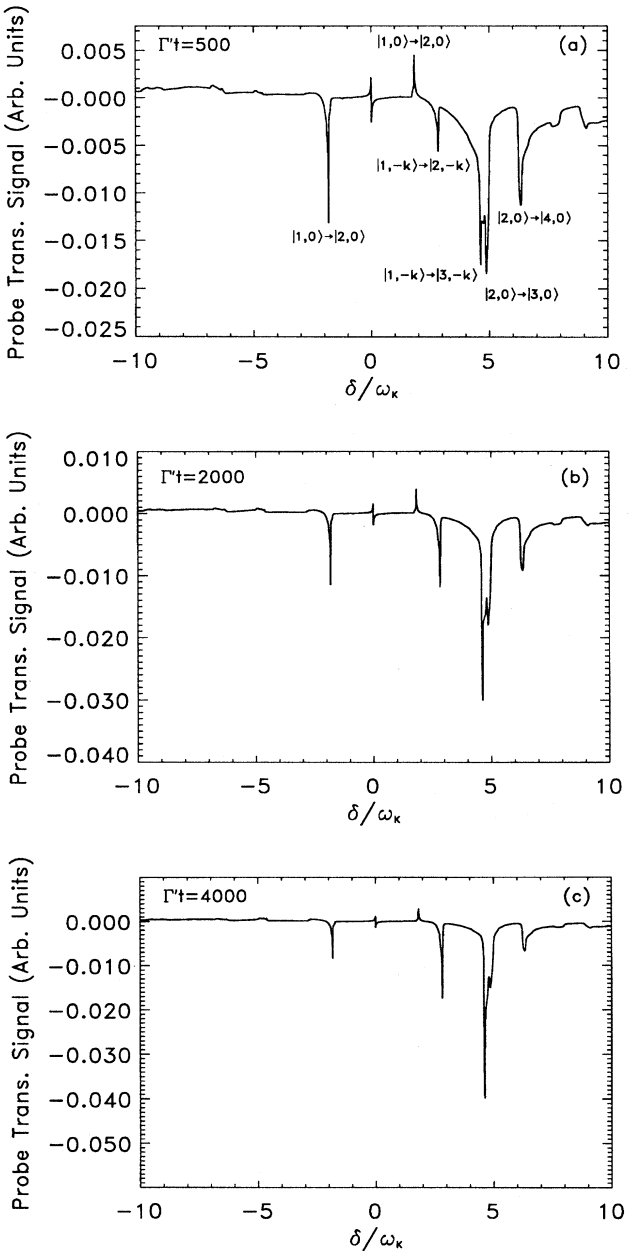

FIG. 1. Calculated probe-transmission spectrum. The potential depth $U_0=50E_k$, and the cooling field detuning $\Delta=20\Gamma$. The cooling time are given by (a) $\Gamma' t=500$, (b) $\Gamma' t=2000$, and (c) $\Gamma' t=4000$. The Bloch states of the Raman transitions are indicated in (a).

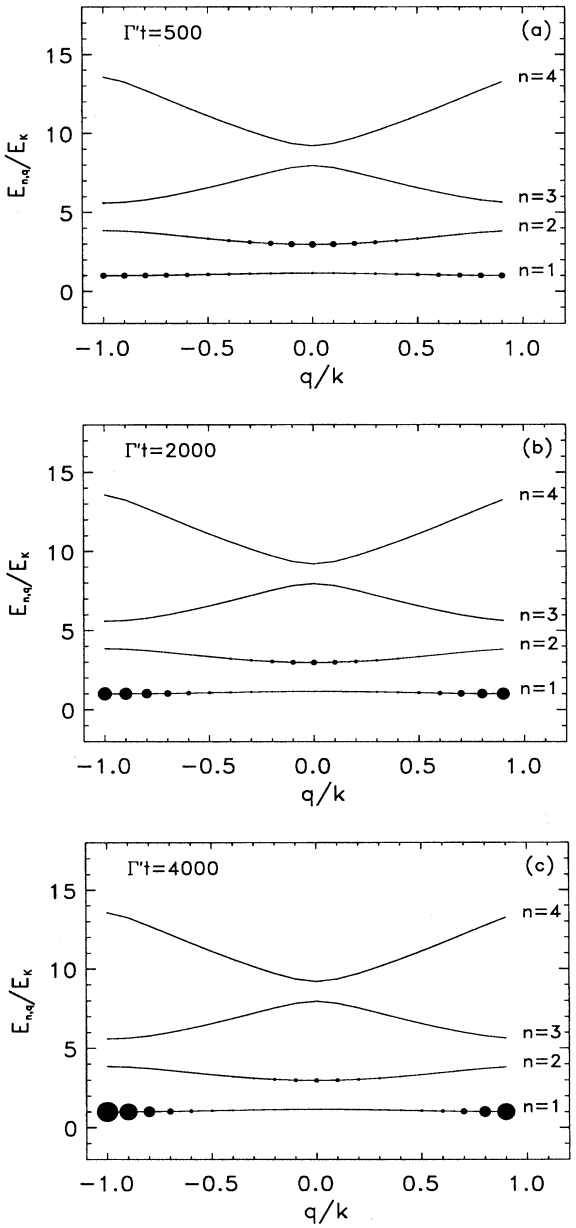

FIG. 2. Eigenenergies of the Bloch states in the lowest four bands. The sizes of the filled circles represent the populations of the discrete Bloch states at time (a) $\Gamma' t=500$, (b) $\Gamma' t=2000$, and (c) $\Gamma' t=4000$.

$=\langle n,q|\rho^{(1)}|n',q\rangle$ can be solved from Eq. (11), and the probe-transmission coefficient $S(\delta)$ can be calculated from Eq. (10). For practical computation of the density matrices $\rho^{(0)}$ and $\rho^{(1)}$, one needs to discretize the Bloch index q by imposing a periodic boundary condition in a box with a size that is large compared to the wavelength λ. We have chosen to discretize q on an interval of $\Delta q=k/10$, i.e., $q_i=-k+i\Delta q$, $i=0,\ldots,19$. The resulting spectrum exhibits complicated resonance peaks at $\delta\neq 0$ due to Raman transitions between Bloch states $|n,q\rangle$ and $|n'\neq n,q\rangle$. These Raman peaks are resolved due to the significant variation of $E_{n,q}$ with q, and also due to the exceedingly narrow linewidths of the individual Raman signals, which are found to be on the order of $0.01\omega_k$, where $\omega_k=E_k/\hbar$ is the recoil frequency and E_k is the recoil energy. As a result, the correct probe-transmission spectrum that can be measured experimentally must be calculated in the limit of $\Delta q\rightarrow 0$.

An interpolation method can be used to obtain such a spectrum, which is described briefly below. It can be shown that an individual peak due to a Raman transition between the Bloch states $|n,q\rangle$ and $|n',q\rangle$ can be described by a Lorentzian as

$$I_{n,n',q}(\delta)=\frac{A_{n,n',q}}{(\delta-\omega_{n,n',q})^2+\gamma^2_{n,n',q}}\ , \qquad (12)$$

where the line shape parameters $(A_{n,n',q},\omega_{n,n',q},\gamma_{n,n',q})$ can be obtained for the discrete values of the Bloch index q_i's by solving the density matrix from Eq. (11). When the discretization interval Δq is sufficiently small, these parameters vary linearly between two discrete Bloch indices q_i and q_{i+1} for a given pair of (n,n'). As a result, one can obtain the values of the parameters $(A_{n,n',q},\omega_{n,n',q},\gamma_{n,n',q})$ for $q_i<q<q_{i+1}$ by a linear interpolation from the values of $(A_{n,n',q_i},\omega_{n,n',q_i},\gamma_{n,n',q_i})$ and $(A_{n,n',q_{i+1}},\omega_{n,n',q_{i+1}},\gamma_{n,n',q_{i+1}})$. The overall Raman signal in the limit of $\Delta q\rightarrow 0$ is then obtained as a normalized sum of these calculated and interpolated Lorentzians. The number of added Lorentzians N_{int} between two adjacent discrete Bloch indices q_i and q_{i+1} should be sufficient such that the overall line shape does not depend on N_{int}.

Figure 1 shows the calculated probe spectra in the limit of $\Delta q\rightarrow 0$, at times given by $\Gamma' t=500$, 2000, and 4000, respectively. A number of narrow Raman peaks, whose widths are much smaller than w_k, can be seen in Fig. 1, and the Bloch states participating in the Raman transitions that contribute to the narrow peaks are identified in Fig. 1(a). There also exists a narrow central Rayleigh signal at $\delta=0$, which exhibits a Lorentzian-type dispersion profile. The positions of sidebands due to transitions between the states $|1,0\rangle$ and $|2,0\rangle$ are reversed, in the sense that probe absorption occurs for $\delta<0$ and amplification for $\delta>0$. One also notices from Fig. 1 that there exists an asymmetry in the amplitudes of the signals for $\delta>0$ and $\delta<0$. The magnitude of the absorption signal at $\delta>0$ is much greater than that of the amplification signal at $\delta<0$, and such a difference becomes greater as the cooling time t increases.

The observed features in Fig. 1 are closely related to the existence of dark and gray states in the lattice. For the cooling configuration considered here, there exists an exact dark state $|1,-k\rangle$ whose decay rate is exactly zero [14]. Eventually all the atomic population will accumulate in this state as the cooling time $t\rightarrow\infty$. Besides this dark state, there also exist some nearly dark or gray states whose decay rates are exceedingly small. In particular, the excited Bloch state $|2\ ,\ 0\rangle$ is a gray state, and population inversion between the states $|1\ ,\ 0\rangle$ and $|2\ ,\ 0\rangle$ can exist for a finite cooling time. Figure 2 shows the eigenenergies $E_{n,q}$ of the lowest motional bands together with the population distribution among the discrete Bloch states at various cooling times t. Population inversion between the Bloch states near $q=0$ in the first and second energy bands can be seen in Fig. 2, and Raman transitions between these states with population inversion lead to absorption peaks at $\delta<0$ and amplification peaks at $\delta>0$ in Fig. 1.

The observed spectral asymmetry in Fig. 1 can also be explained based on the existence of dark or gray states. To be specific, let us look at the Raman transitions between a ground state $|1\ ,\ q\rangle$ and the excited states $|n\ ,\ q\rangle$ with $n\neq 1$. Suppose that $|1\ ,\ q\rangle$ is a dark or gray state with respect to the cooling field, whose population is greater than those of the excited states. In the case of $\delta=\omega'-\omega<0$, a Raman transition from $|1\ ,\ q\rangle$ to $|n\ ,\ q\rangle$ involves the absorption of a cooling field photon and the emission of a probe field photon. Since $|1\ ,\ q\rangle$ is a dark or gray state, the probability for atoms in this state to absorb a photon from the cooling field is zero or quite small. As a result, the magnitude of the Raman signal becomes suppressed in this case. On the other hand, it is still possible for the atoms in $|1,\ q\rangle$ to absorb photons from the probe field, and in the case of $\delta>0$, the processes of absorbing probe field photons and emitting cooling field photons lead to the absorption Raman signal in Fig. 1.

As the cooling time t increases, more and more atoms will be accumulated in the dark state $|1,-k\rangle$, and the amplitude of Raman peaks associated with this dark state increases, while other Raman peaks decrease in magnitude, as is evident from Fig. 1. The strength of the central Rayleigh signal also decreases as the cooling time increases, since the atoms in the dark state do not contribute to this signal. Therefore, by monitoring the amplitudes of the Raman and Rayleigh signals, one can obtain information on the accumulation of the dark-state population in the lattice.

In this paper, the probe-transmission spectrum of a 1D blue-detuned lattice is calculated. The main features of the probe transmission spectrum shown above, including narrow line widths, reversed amplification-absorption features, and the signal asymmetry for $\delta<0$ and $\delta>0$ are characteristic of the blue-detuned lattices where dark or gray states can exist. One expects similar features to be found in the cases of 2D or 3D lattices.

J.G. is supported by the Condon Fellowship fund at JILA. J.C. is supported in part by NSF Grant No. PHY90-12244 through the University of Colorado.

[1] P. Verkerk *et al.*, Phys. Rev. Lett. **68**, 3861 (1992).
[2] A. Hemmerich and T. W. Hänsch, Phys. Rev. Lett. **70**, 410 (1993).
[3] G. Grynberg *et al.*, Phys. Rev. Lett. **70**, 2249 (1993).
[4] A. Hemmerich, C. Zimmermann, and T. W. Hänsch, Phys. Rev. Lett. **72**, 625 (1994).
[5] A. Kastberg *et al.*, Phys. Rev. Lett. **74**, 1542 (1995).
[6] A. Hemmerich, M. Weidemüller, and T. Hänsch, Europhys. Lett. **27**, 427 (1994).
[7] D. R. Meacher *et al.*, Phys. Rev. Lett. **74**, 1958 (1995).
[8] J.-Y. Courtois and G. Grynberg, Phys. Rev. A **46**, 7060 (1992).
[9] J. Guo, Phys. Rev. A **49**, 3934 (1994); **51**, 2338 (1995).
[10] J. Guo, Phys. Rev. A (to be published).
[11] G. Grynberg and J.-Y. Courtois, Europhys. Lett. **27**, 41 (1994); A. Hemmerich *et al.*, Phys. Rev. Lett. **75**, 37 (1995).
[12] A. Aspect *et al.*, J. Opt. Soc. Am. B **6**, 2112 (1989).
[13] M. S. Shahriar *et al.*, Phys. Rev. A **48**, R4035 (1993).
[14] P. Marte *et al.*, Phys. Rev. A **49**, 4826 (1994).